

Modified Implicit Discretization of the Super-Twisting Controller

Benedikt Andritsch, Lars Watermann, Stefan Koch, Markus Reichhartinger, Johann Reger,
and Martin Horn

Abstract—In this paper a novel discrete-time realization of the super-twisting controller is proposed. The closed-loop system is proven to converge to an invariant set around the origin in finite time. Furthermore, the steady-state error is shown to be independent of the controller gains. It only depends on the sampling time and the unknown disturbance. The proposed discrete-time controller is evaluated comparative to previously published discrete-time super-twisting controllers by means of the controller structure and in extensive simulation studies. The continuous-time super-twisting controller is capable of rejecting any unknown Lipschitz-continuous perturbation and converges in finite time. Furthermore, the convergence time decreases, if any of the gains is increased. The simulations demonstrate that the closed-loop systems with each of the known controllers lose one of these properties, introduce discretization-chattering, or do not yield the same accuracy level as with the proposed controller. The proposed controller, in contrast, is beneficial in terms of the above described properties.

Index Terms—Backward Euler discretization, Discrete-time control, Implicit discretization, Sliding mode control, Super-twisting algorithm, Super-twisting control

I. INTRODUCTION

The field of Sliding Mode (SM) Control (SMC) has proven to be of high importance when considering systems with unknown disturbances [1]. In continuous-time, SMC manages to completely reject any disturbances that fulfill some requirements like boundedness or Lipschitz-continuity. However, SM controllers are mostly implemented on discrete-time hardware, requiring appropriate representations of these controllers. Discrete-time SM controllers have to deal with unpleasant effects like discretization-chattering, which diminishes the advantageous properties of SMC [2], [3]. One

This work has been submitted to the IEEE for possible publication. Copyright may be transferred without notice, after which this version may no longer be accessible.

The financial support by the Austrian Science Fund (FWF) grant no. I 4152, the Austrian Federal Ministry for Digital and Economic Affairs, the National Foundation for Research, Technology and Development and the Christian Doppler Research Association is gratefully acknowledged. The second and fifth author further acknowledge the financial support by the German Research Foundation (DFG), project no. 416911519, and by the European Union Horizon 2020 research and innovation program under Marie Skłodowska-Curie grant no. 824046.

B. Andritsch and M. Reichhartinger are with the Institute of Automation and Control at Graz University of Technology, Graz, Austria. (email: benedikt.andritsch@tugraz.at, markus.reichhartinger@tugraz.at)

S. Koch and M. Horn are with the Christian Doppler Laboratory for Model-Based Control of Complex Test Bed Systems, Institute of Automation and Control, Graz University of Technology, Graz, Austria. (email: stefan.koch@tugraz.at, martin.horn@tugraz.at)

L. Watermann and Johann Reger are with the Control Engineering Group at Technische Universität Ilmenau, Ilmenau, Germany. (email: lars.watermann@tu-ilmenau.de, johann.reger@tu-ilmenau.de)

of the first techniques in conventional SMC [1] avoiding discretization-chattering is the implicit discretization [4].

A famous continuous-time SM system is the Super-Twisting Algorithm (STA) [5], [6]. The STA is capable of rejecting Lipschitz-continuous disturbances, which is of high interest in real-world control problems [7], [8]. Therefore, a proper discrete-time implementation of the Super-Twisting Controller (STC) is essential for many applications. There have been different approaches to achieve an implicitly discretized version of the STC [9], [10]. Also, non-implicit discretization techniques can be applied to the STC, e.g. the matching approach [11] and the low-chattering discretization [12].

The continuous-time STC has the following properties:

- reject Lipschitz-continuous perturbations [5],
- finite-time convergence [5] and
- increasing any controller parameter reduces the convergence time [13].

Furthermore, the following are desired properties of the discrete-time controller:

- no discretization-chattering occurs, i.e. the control error vanishes when no disturbance and no measurement noise are present,
- the steady-state error, i.e. the control error after all transients died out, is proportional to the discretization time squared, as in [14], and
- the steady-state accuracy is insensitive to controller parameters.

With the last property, the controller parameters can be selected solely on requirements regarding convergence time and control signal magnitude, and do not have to consider a trade-off with the accuracy of the controller. Each of the existing discretizations of the STC fails to resemble some of these properties. Therefore, in this paper a novel discretization of the STC is presented, that unites all above-mentioned features. Measurement noise is not investigated in this paper.

At first, an overview of existing discrete-time versions of the STC is given in Section II. Then, in Section III a novel implicit discretization of the STC is presented. Further, stability properties of the presented discretization are analyzed. Finally, in extensive simulation studies in Section IV it is demonstrated that the proposed controller preserves all crucial properties of the continuous-time STC, in contrast to previously published controllers.

Mathematical Notations

Let

$$\text{sign}(x) \in \begin{cases} \{1\} & \text{if } x > 0, \\ \{-1\} & \text{if } x < 0, \\ [-1, 1] & \text{if } x = 0 \end{cases}$$

be the signum function with $x \in \mathbb{R}$. Furthermore, the signed power function $\lfloor x \rfloor^y = \text{sign}(x) |x|^y$, with $x, y \in \mathbb{R}$ will be used. Note that $\lfloor x \rfloor^0 = \text{sign}(x)$. Finally, let $\text{sat}(x) = \begin{cases} x & \text{if } |x| < 1 \\ \text{sign}(x) & \text{else} \end{cases}$ be the saturation function.

II. RELATED WORK

The STC considers the dynamics of the sliding variable x_1 with relative degree 1 of an affine-input dynamic system [5], [15], i.e.

$$\begin{aligned} \dot{x}_1 &= u + \varphi, \\ \dot{\varphi} &= \Delta. \end{aligned} \quad (1)$$

System (1) is denoted as plant and x_1 and the perturbation φ as plant states in the following. The remaining terms are the control signal u and the Lebesgue-measurable unknown disturbance $\Delta(t)$ with $|\Delta(t)| < L \forall t$ and some known constant L . Due to the bounded derivative φ is Lipschitz-continuous.

The dynamic sliding-mode controller

$$\begin{aligned} u &= -\alpha \lfloor x_1 \rfloor^{\frac{1}{2}} + v, \\ \dot{v} &= -\beta \lfloor x_1 \rfloor^0, \end{aligned} \quad (2)$$

with the controller state v is known as STC and stabilizes $x_1 = 0$ of (1) if the constant gains α and $\beta > L$ are chosen accordingly [5]. The closed-loop system

$$\begin{aligned} \dot{x}_1 &= -\alpha \lfloor x_1 \rfloor^{\frac{1}{2}} + x_2, \\ \dot{x}_2 &= -\beta \lfloor x_1 \rfloor^0 + \Delta, \end{aligned} \quad (3)$$

with $x_2 = \varphi + v$ resulting from the plant (1) and the STC (2) is called STA.

The goal of implementing the STC is to determine a discrete-time representation of the controller (2), which can generally be written as

$$\begin{aligned} u_k &= -\alpha \Psi_1(x_{1,k}) + v_{k+1}, \\ v_{k+1} &= v_k - h\beta \Psi_2(x_{1,k}), \end{aligned} \quad (4)$$

with the state dependent functions Ψ_1 and Ψ_2 , the constant discretization-time h , the known discrete-time system state $x_{1,k} = x_1(kh)$, and $k = 1, 2, \dots$. Note that measurement noise in the state $x_{1,k}$ is not investigated in this paper. The discrete-time control variable u_k is then fed to the continuous-time system through a zero-order hold element, i.e. $u(t) = u_k$ for $kh \leq t < (k+1)h$. Note that u_k contains the controller-state at $k+1$, i.e. v_{k+1} , as in this paper mainly implicit discretization approaches are considered. Denote by \mathcal{C}_* the controller resulting from (4) and specific controller functions $\Psi_{1,*}$ and $\Psi_{2,*}$. In the following, several discrete-time realizations of the STC are presented.

A. Implicit Discretization

One discrete-time STC was published in [9], [16] by Brogliato *et al.* and can be written as

$$\begin{aligned} \Psi_{1,\text{Brogliato}} &= \\ &= \text{sign}(x_{1,k}) \left(-\frac{h\alpha}{2} + \sqrt{\frac{h^2\alpha^2}{4} + \max(0, |x_{1,k} + hv_k| - h^2\beta)} \right), \\ \Psi_{2,\text{Brogliato}} &= \text{sat}\left(\frac{x_{1,k} + hv_k}{h^2\beta}\right). \end{aligned} \quad (5)$$

Note that $\Psi_{1,\text{Brogliato}}$ depends not only on the plant state $x_{1,k}$, but also on the controller state v_k . The authors use an implicit discretization approach to establish the explicitly given discrete-time controller functions (5). It is proven that the undisturbed closed-loop system is globally asymptotically stable. The authors introduce the sliding variable $x_{1,k} + hv_k$, which is driven to zero and maintained there. Also, $\mathcal{C}_{\text{Brogliato}}$ drives the closed-loop state $\varphi_k + v_k$ to zero.

However, let us assume an unbounded perturbation φ_k , e.g. due to a constant disturbance Δ_k . Then φ_k will grow, and thus, also v_k will grow. With the sliding variable kept at the origin, therefore also $x_{1,k}$ will grow and the control goal $x_{1,k} = 0$ can not be maintained. Therefore, the controller $\mathcal{C}_{\text{Brogliato}}$ is not able to reject an unbounded perturbation φ , which reduces the class of disturbances Δ that can be handled by the controller compared to the continuous-time STC. These thoughts will be discussed in simulations in Section IV as well.

B. Discretization Based on Matching Approach

Another discrete-time implementation of the controller (2) is presented in [11], [17] by Koch *et al.* The authors utilize the matching approach to establish a discrete-time controller, resulting in the controller functions

$$\begin{aligned} \Psi_{1,\text{Koch}} &= -\frac{1}{\alpha h} \left(e^{\frac{p_1 h}{\sqrt{|x_{1,k}|}}} + e^{\frac{p_2 h}{\sqrt{|x_{1,k}|}}} - 2 \right) x_{1,k} - \frac{h\beta}{\alpha} \Psi_{2,\text{Koch}}, \\ \Psi_{2,\text{Koch}} &= \frac{1}{h^2\beta} \left(e^{\frac{p_1 h}{\sqrt{|x_{1,k}|}}} - 1 \right) \left(e^{\frac{p_2 h}{\sqrt{|x_{1,k}|}}} - 1 \right) x_{1,k}, \end{aligned} \quad (6)$$

with $p_{1,2} = -\frac{\alpha}{2} \pm \sqrt{\frac{\alpha^2}{4} - \beta}$. The discrete-time closed-loop system is shown to avoid discretization-chattering effects and to be globally asymptotically stable in the disturbance-free case. Note that $\Psi_{1,\text{Koch}}$ differs from the function in [11] due to the different definition of the general discrete-time controller (4).

C. Semi-Implicit Discretization

The third known discrete-time version of the STC that is considered in this paper was published in [10] by Xiong *et al.* and is obtained by a semi-implicit discretization. It consists of the controller functions

$$\begin{aligned} \Psi_{1,\text{Xiong}} &= \frac{1}{h\alpha} D_k \text{sat}\left(\frac{x_{1,k}}{D_k}\right), \\ \Psi_{2,\text{Xiong}} &= \text{sat}\left(\frac{x_{1,k}}{D_k}\right), \end{aligned} \quad (7)$$

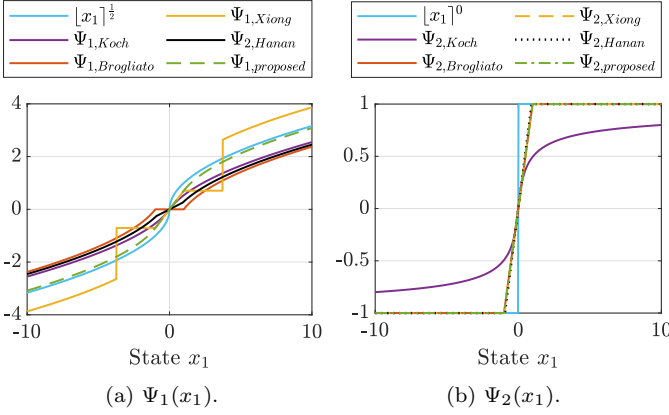


Fig. 1: Compared controller functions.

where $D_k = \begin{cases} h\alpha|x_{1,k}|^{\frac{1}{2}} + h^2\beta & \text{if } |x_{1,k}| > h\alpha|x_{1,k}|^{\frac{1}{2}} + h^2\beta \\ h^2\beta & \text{else.} \end{cases}$

The authors show that the controller is insensitive to an overestimation of the gains regarding the asymptotic accuracy of the closed-loop system.

D. Low-Chattering Discretization

Finally, the last considered discrete-time STC is derived from the low-chattering differentiator presented in [12]. The controller functions take the form

$$\begin{aligned} \Psi_{1,\text{Hanan}} &= \text{sat} \left(\frac{|x_{1,k}|}{\gamma h^2} \right)^{\frac{1}{2}} [x_{1,k}]^{\frac{1}{2}} - \frac{h\beta}{\alpha} \text{sat} \left(\frac{x_{1,k}}{\gamma h^2} \right), \\ \Psi_{2,\text{Hanan}} &= \text{sat} \left(\frac{x_{1,k}}{\gamma h^2} \right). \end{aligned} \quad (8)$$

The derivation of this discrete-time representation of the STC and the selection of γ are given in Appendix A.

Fig. 1a and 1b show the discrete-time controller functions $\Psi_{1,j}(x_1)$ respective $\Psi_{2,j}(x_1)$ from (5), (6), (7) and (8) with $j \in \{\text{Brogliato, Koch, Xiong, Hanan}\}$, as well as the functions $[x_1]^{\frac{1}{2}}$ respective $[x_1]^0$ from the continuous-time controller (2). The parameters were chosen as $h = 1$, $\beta = 1$, $\alpha = \sqrt{2}\beta$. For the computation of $\Psi_{1,\text{Brogliato}}(x_1)$ and $\Psi_{2,\text{Brogliato}}(x_1)$, v_k was assumed to be zero. This is the case in steady state in the absence of a disturbance. Fig. 1a shows two regions within x_1 , where $\Psi_{1,\text{Xiong}}$ is constant. Between these regions, $\Psi_{1,\text{Xiong}}$ is linear. The size of the constant regions depends on the parameters α and β and is large w.r.t. the linear region, when α is large compared to β . The effect of this linear region will be discussed in Section IV. Note that Fig. 1 helps to get an intuitive understanding of the controllers.

III. PROPOSED DISCRETE-TIME STC

Sampling the continuous-time state $x_1(t)$ of system (1) with $u(t) = u_k \forall t \in [kh, (k+1)h)$ results in $x_1((k+1)h) = x_1(kh) + hu_k + \int_{kh}^{(k+1)h} \varphi(\tau) d\tau$. Defining the discrete-time

state $\varphi_k := \frac{1}{h} \int_{kh}^{(k+1)h} \varphi(\tau) d\tau$ and the unknown discrete-time input $\Delta_k := \frac{1}{h}(\varphi_{k+1} - \varphi_k)$ yields

$$\begin{aligned} \Delta_k &= \frac{1}{h^2} \left(\int_{(k+1)h}^{(k+2)h} \varphi(\tau) d\tau - \int_{kh}^{(k+1)h} \varphi(\tau) d\tau \right) \\ &= \frac{1}{h^2} \int_{kh}^{(k+1)h} \varphi(\tau + h) - \varphi(\tau) d\tau. \end{aligned} \quad (9)$$

As $|\dot{\varphi}(t)| = |\Delta(t)| \leq L \forall t > 0$, $|\varphi(t+h) - \varphi(t)| \leq Lh$ holds and thus $|\Delta_k| \leq L$. Defining $x_{1,k} := x_1(kh)$ yields the discrete-time plant model

$$\begin{aligned} x_{1,k+1} &= x_{1,k} + hu_k + h\varphi_k, \\ \varphi_{k+1} &= \varphi_k + h\Delta_k. \end{aligned} \quad (10)$$

The state φ_k can be interpreted as the mean value of $\varphi(t)$ in the interval $t \in [kh, (k+1)h)$. Also, φ_k as well as Δ_k are virtual values, and not samples of the continuous-time signals $\Delta(t)$ and $\varphi(t)$. Note that even though (10) is structurally equivalent to an Euler forward discretization of (1) the state $x_{1,k}$ coincides with the samples $x_1(kh)$.

The novel discrete-time STC functions

$$\begin{aligned} \Psi_{1,\text{proposed}} &= \text{sign}(x_{1,k}) \left(\frac{h\beta}{\alpha} \text{sat} \left(\frac{|x_{1,k}|}{h^2\beta} \right) - \frac{h\alpha}{2} + \sqrt{\frac{h^2\alpha^2}{4} + \max(0, |x_{1,k}| - h^2\beta)} \right), \\ \Psi_{2,\text{proposed}} &= \text{sat} \left(\frac{x_{1,k}}{h^2\beta} \right) \end{aligned} \quad (11)$$

are proposed in this paper for the discrete-time plant model (10). It is worth noting that the controller functions (11) resemble the terms of the implicit controller functions (5), with $x_{1,k} + hv_k$ replaced by $x_{1,k}$, and extended by the saturation term in the first equation. The controller can therefore be regarded as a modified implicitly discretized STC. Fig. 1a and 1b also show the controller functions in (11). Note that $\Psi_{2,\text{proposed}}$, $\Psi_{2,\text{Brogliato}}$ and $\Psi_{2,\text{Xiong}}$ coincide. Furthermore, $\Psi_{1,\text{proposed}}$ and $\Psi_{1,\text{Xiong}}$ coincide near the origin, i.e. at $|x_1| \leq h^2\beta$.

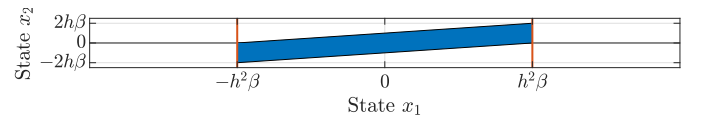


Fig. 2: Invariant set \mathcal{M} of the closed-loop system.

Let the unknown virtual state $x_{2,k}$ be defined as $x_{2,k} := v_k + \varphi_k$. The closed-loop system resulting from the discrete-time plant (10) and the controller $\mathcal{C}_{\text{proposed}}$ is

$$\begin{aligned} x_{1,k+1} &= x_{1,k} - 2h^2\beta \text{sat} \left(\frac{x_{1,k}}{h^2\beta} \right) - h\alpha \text{sign}(x_{1,k}) \left(-\frac{h\alpha}{2} + \sqrt{\frac{h^2\alpha^2}{4} + \max(0, |x_{1,k}| - h^2\beta)} \right) + hx_{2,k}, \\ x_{2,k+1} &= x_{2,k} - h\beta \text{sat} \left(\frac{x_{1,k}}{h^2\beta} \right) + h\Delta_k. \end{aligned} \quad (12)$$

In the following, the stability properties of the discrete-time STA (12) are examined. For this define $\mathcal{M} = \{(x_{1,k}, x_{2,k}) \in$

$\mathbb{R}^2 \{ |x_{1,k}| \leq h^2\beta, |hx_{2,k} - x_{1,k}| \leq h^2\beta \}$. \mathcal{M} is plotted in Fig. 2 in state-space as a blue area.

Proposition 1. Consider the closed-loop system (12) with the Lipschitz constant L , i.e. $|\Delta_k| \leq L \forall k$, and $\beta > L$. Then \mathcal{M} is a forward invariant set and if $x_k \in \mathcal{M}$ is fulfilled for some $k = K$, the steady-state error is limited, i.e. $\limsup_{k \geq K+2} |x_{1,k}| \leq h^2L$. Further, the closed-loop system is exact in the absence of a disturbance, i.e. the state $x_{1,k}$ converges to zero. Thus, discretization-chattering is completely avoided.

Proof. Assume $|x_{1,k}| \leq h^2\beta$. Then the controller (4) with (11) can be simplified to

$$\begin{aligned} u_k &= -\frac{1}{h}x_{1,k} + v_{k+1}, \\ v_{k+1} &= v_k - \frac{1}{h}x_{1,k}, \end{aligned} \quad (13)$$

which in explicit form yields $u_k = -\frac{2}{h}x_{1,k} + v_k$.

The second-order closed-loop system resulting from (10) and (13) in matrix-form is then given by

$$\begin{bmatrix} x_{1,k+1} \\ x_{2,k+1} \end{bmatrix} = \underbrace{\begin{bmatrix} -1 & h \\ -\frac{1}{h} & 1 \end{bmatrix}}_M \begin{bmatrix} x_{1,k} \\ x_{2,k} \end{bmatrix} + \begin{bmatrix} 0 \\ h \end{bmatrix} \Delta_k. \quad (14)$$

The eigenvalues of the system-matrix M are both zero, which means that (14) is a second-order dead-beat system [18]. Thus, the steady state is reached after two steps.

The discrete-time controller acts as a dead-beat controller, whenever $|x_{1,k}| \leq h^2\beta$. In order to reach steady state, the dead-beat controller (13) must be applied to the plant two times consecutively. Thus, to reach steady state $|x_{1,k}| \leq h^2\beta$ and $|x_{1,k+1}| \leq h^2\beta$ must hold. According to (14) $|x_{1,k+1}| \leq h^2\beta \Leftrightarrow |hx_{2,k} - x_{1,k}| \leq h^2\beta$, which corresponds to $x_k \in \mathcal{M}$. Assume $x_K \in \mathcal{M}$. Then (14) gives $|x_{1,K+2}| = |-x_{1,K+1} + hx_{2,K+1}| = |-(x_{1,K} + hx_{2,K}) + (-x_{1,K} + hx_{2,K}) + h^2\Delta_K| = |h^2\Delta_K| \leq h^2L < h^2\beta$. Therefore, \mathcal{M} is forward invariant for system (12) and $x_{1,K+2+i} = h^2\Delta_{K+i} \forall i \geq 0$. \square

Theorem 2. Let $L \geq 0$, $|\Delta_k| \leq L \forall k$, $V > 0$ and discretization time $h > 0$. Given parameters $\alpha > 0$, $\beta > \max\left(4L, \frac{5}{7}\frac{\sqrt{V}}{h}, \sqrt{L^2 + \frac{2L\sqrt{V}}{h^2}}\right)$, and initial states $(x_{1,0}, x_{2,0})$ fulfilling $V \geq V_0 := 2\beta|x_{1,0} - hx_{2,0}| + x_{2,0}^2$. Then, the states of system (12) converge to the set \mathcal{M} in finite time and remain there. Further, in the absence of a disturbance, i.e. $L = 0$, and if $\alpha > 0$, $\beta > 0$ the origin of system (12) is globally finite-time stable.

The proof of Theorem 2 is in Appendix B. \square

IV. EVALUATION IN SIMULATION STUDIES

In this section, the results of numerical simulations are presented. All simulations were performed in MATLAB®/Simulink®. The plant was simulated in discrete-time according to (10) with the same discretization-time h as the controllers. The discrete-time disturbance Δ_k for the simulations was computed solving the integral in (9) analytically yielding $x_k = x(hk)$. The simulations were

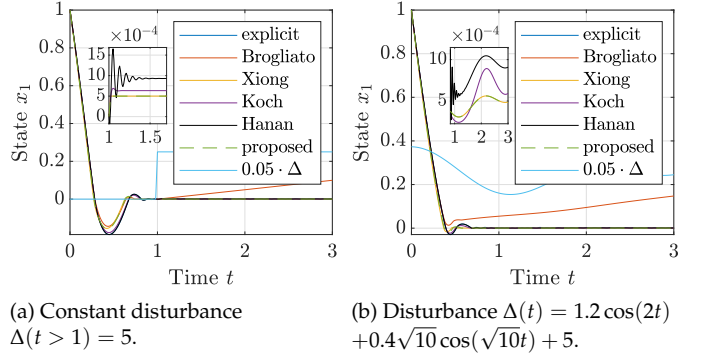


Fig. 3: Simulation in time-domain with a disturbance, $\alpha = \sqrt{10}$, $\beta = 10$, $h = 0.01$ and $x_1(0) = 1$.

performed with a fixed-step solver. In the following, Σ_* denotes the simulated closed-loop system consisting of the plant and the discrete-time controller \mathcal{C}_* . It is shown in what regard $\mathcal{C}_{\text{proposed}}$ is an improvement to state-of-the-art discrete-time STCs.

A. Disturbed Case

The first simulation was performed with a constant disturbance $\Delta = 1 \forall t \geq 1$ and $\Delta = 0 \forall t < 1$. The parameters were chosen as $\alpha = \sqrt{10}$, $\beta = 10$, the discretization time $h = 0.01$ and $x_1(0) = 1$. The second simulation was performed with the same parameters and a disturbance known from literature [10], [17] with a constant offset of 5, $\Delta(t) = 1.2 \cos(2t) + 0.4\sqrt{10} \cos(\sqrt{10}t) + 5$. The results are presented in Fig. 3a and 3b. The results clearly show that $\mathcal{C}_{\text{Brogliato}}$ is not capable of rejecting constant parts of the disturbance Δ , as it was described in Section II. All other controllers result in a state x_1 converging close to zero. $\mathcal{C}_{\text{Hanan}}$ leads to decaying oscillations in x_1 .

B. Undisturbed Case

Three more simulations were performed with no disturbance, i.e. $\Delta \equiv 0$. In Fig. 4a $\alpha = \sqrt{10}$ was chosen as before. In Fig. 4b the parameter was set to $\alpha = 30$, which is large w.r.t. β , and in Fig. 4c $\alpha = 1.5\sqrt{\beta/1.1}$ was set according to the recommended parameter choice for $\mathcal{C}_{\text{Hanan}}$ in [12, Fig. 3]. The other parameters remained unchanged, i.e. $\beta = 10$, discretization time $h = 0.01$ and $x_1(0) = 1$. The state x_1 is depicted in absolute values and scaled logarithmically in these plots, in order to emphasize the differences between the results of the controllers. The results show that Σ_{explicit} is not exact and exhibits discretization-chattering in steady state. All other systems converge to zero without discretization-chattering effects. However, Σ_{Hanan} converges slower than the other systems. From the continuous-time STA (3) it is expected that increasing the parameter α leads to faster convergence times. However, increasing α from $\sqrt{10}$ to 30 in Fig. 4b shows an increased convergence time of Σ_{Xiong} . The systems Σ_{proposed} and $\Sigma_{\text{Brogliato}}$ converge faster to zero. System Σ_{Koch} exhibits a larger convergence time than Σ_{proposed} and $\Sigma_{\text{Brogliato}}$.

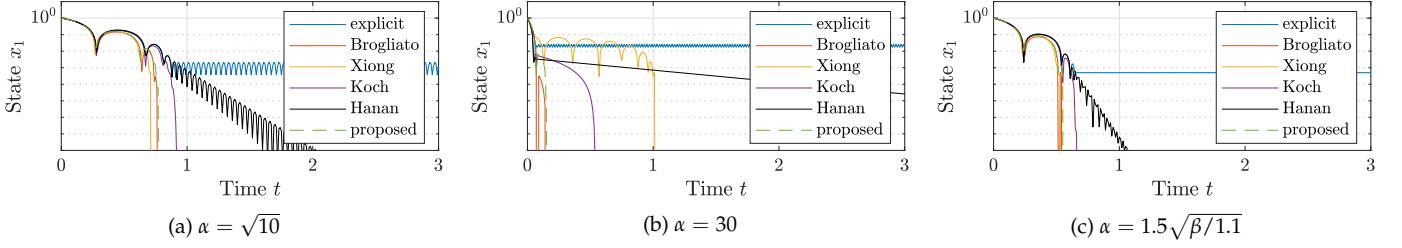


Fig. 4: Simulations in time-domain in the undisturbed case, $\beta = 10$, $h = 0.01$ and $x_1(0) = 1$.

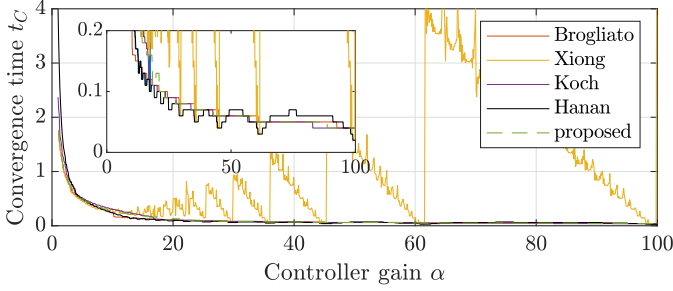


Fig. 5: Convergence time t_C over varying parameter α .

C. Convergence Time when Varying One Parameter

In order to analyze the behavior of increasing convergence times when increasing α , the convergence time was determined for several parameter values α . The displayed convergence time t_C is the lowest time for which the absolute state value does not exceed 1% of the initial value, i.e. $|x_1(t)| \leq 10^{-2}|x_1(0)| \forall t \geq t_C$. Fig. 5 shows the convergence times of the compared systems over the parameter α , which was set to values between 1 and 100, i.e. 0.1β and 10β , in intervals of 0.1. The other parameters were fixed at $\beta = 10$, $h = 0.01$ and $x_1(0) = 1$. Fig. 5 illustrates that the convergence time of Σ_{Xiong} behaves very sensitive to changes in α when $\alpha > \beta$. Small changes in α can lead to a large increase of the convergence time, e.g. changing α from 29.8 to 29.9 results in t_C changing from 0.11 to 0.87 (all numbers are rounded). The reason for the large convergence times of Σ_{Xiong} when $\alpha > \beta$ may be connected to the constant regions of the controller function $\Psi_{1,\text{Xiong}}$ in (7) which is depicted in Fig. 1a. When α is large w.r.t. β , then the constant regions are larger w.r.t. the linear region of $\Psi_{1,\text{Xiong}}$, as described in Section II. The function $\Psi_{1,\text{Xiong}}$ can be interpreted as a rate at which x_1 approaches the origin. When this function is constant with a rather small magnitude, this approaching phase could then take longer, the larger this constant region is. Σ_{Hanan} shows oscillations in the convergence time with very small magnitude, interestingly with a similar frequency as the oscillations in Σ_{Xiong} .

D. Steady-State Accuracy when Varying the Parameters

Finally, simulations were performed regarding the accuracy of the closed-loop systems, i.e. the remaining steady-state error. Let this steady-state error be defined as $e_f = \limsup_t |x_1|$, with the initial value $x_1(0) = 0$. The systems were simulated until $t = 20$. The disturbance was chosen

as $\Delta(t) = 1.2 \cos(2t) + 0.4\sqrt{10} \cos(\sqrt{10}t)$, which was also used in [10], [17]. The discretization time was set to $h = 0.05$. Fig. 6a depicts e_f over the value Λ , which determines the parameters $\alpha = 1.5\sqrt{\Lambda}$ and $\beta = 1.1\Lambda$. This parameter relation corresponds to the suggested parameter choice in [12] and was also applied in [10], where the same simulation was performed. The value Λ was varied between 1 and 40 in 1000 steps. The results from [10] were reproduced, whereas Σ_{proposed} and Σ_{Hanan} performed very similar to Σ_{Xiong} . Fig. 6b and 6c show e_f over varying α and β from 1 to 80 and 110, respectively, in 1000 steps. The second controller parameter was fixed at 10. The results again show the exactness of Σ_{proposed} as well as Σ_{Xiong} , which yield the same small steady-state error after some minimal gain values. The system $\Sigma_{\text{Brogliato}}$, however, settles at larger errors, due to the appearance of the attenuated perturbation φ in x_1 in steady state. In the results of Σ_{Koch} , which is not the result of an implicit approach, a dependency between the controller parameters α and β and the steady-state error can be observed. Increasing α even drives the steady-state error of Σ_{Koch} to the same level where $\Sigma_{\text{Brogliato}}$ settles, as can be seen in Fig. 6b. The system Σ_{Hanan} achieves smaller steady-state errors than Σ_{proposed} and Σ_{Xiong} within some bounds of α and β . Outside of these bounds, the accuracy of Σ_{Hanan} decreases significantly.

E. State Trajectories

Figure 7 shows the state trajectories of the proposed algorithm with various discretization times h comparative to the continuous-time algorithm. In this simulation, the input $\Delta \equiv 0$ and the parameters were selected as $\alpha = \sqrt{10}$, $\beta = 10$, $x_{1,0} = 1$, $x_{2,0} = 0$ and $h \in \{0.01, 0.05, 0.1\}$. The continuous-time trajectory was established with an Euler forward discretized STC and a discretization time of 10^{-5} . In this simulation Σ_{proposed} yields results similar to the continuous-time trajectory for small h .

V. CONCLUSION

In this paper, a novel discrete-time super-twisting controller is presented. It is shown to converge to an invariant set in finite time. Additionally, the absence of any discretization-chattering effects is shown. The controller is directly compared to previously published discrete-time super-twisting controllers analytically regarding the controller structure as well as in simulation studies. The analytic considerations and simulations showed that the presented controller resembles best several properties of the continuous-time controller. The proposed

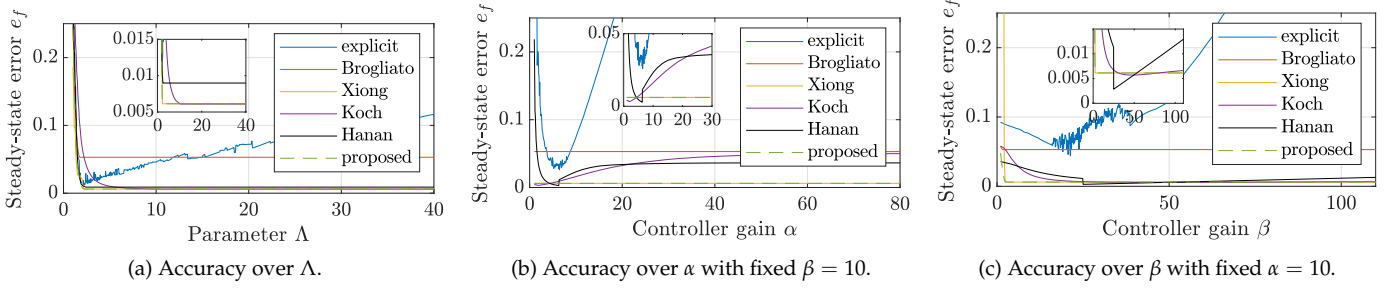


Fig. 6: Accuracy by means of the steady-state error e_f , $h = 0.05$ and $x_1(0) = 0$.

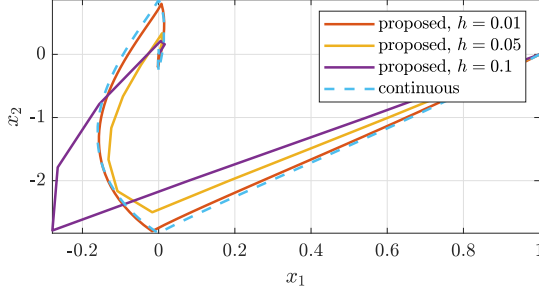


Fig. 7: State trajectories with $\Delta \equiv 0$.

discretization can handle all Lipschitz-continuous perturbations. Further, its finite convergence time decreases when any of the controller gains is increased. Moreover, the presented controller yields a steady-state error that is independent of the controller gains and it introduces no discretization-chattering effects. The proposed discrete-time super-twisting controller unites all of these beneficial properties, in contrast to the known controllers. In future work, the presented controller will be applied to real-world problems.

APPENDIX A

DERIVATION OF THE LOW-CHATTERING DISC.

The discrete-time differentiator according to [12] with a differentiation order of 1 and a filtering order of 0 is given by

$$\begin{aligned} z_{0,k+1} &= z_{0,k} + h z_{1,k} - h \tilde{\lambda}_1 \hat{L}^{\frac{1}{2}} [z_{0,k} - f_{0,k}]^{\frac{1}{2}} \\ z_{1,k+1} &= z_{1,k} - h \tilde{\lambda}_0 \hat{L} [z_{0,k} - f_{0,k}]^0, \end{aligned} \quad (15)$$

where $f_{0,k}$ is the discrete-time signal to be differentiated, $\tilde{\lambda}_1$ and $\tilde{\lambda}_0$ are constant parameters and $z_{0,k}$ and $z_{1,k}$ are the observer states that estimate the signal $f_{0,k}$ and its first derivative $f_{1,k}$, respectively. Further, \hat{L} is an adaptive parameter following the computation law $\hat{L} = L \cdot \text{sat}\left(\frac{|z_{0,k} - f_{0,k}|}{L k_L h^2}\right)$, with L being the known Lipschitz constant of the unknown signal $f_{1,k}$ and a constant parameter k_L . Selecting $\tilde{\lambda}_0 L = \beta$, $\tilde{\lambda}_1 L^{\frac{1}{2}} = \alpha$ and $L k_L = \gamma$ yields the error dynamics of the differentiator (15)

$$\begin{aligned} x_{1,k+1} &= x_{1,k} + h x_{2,k} - h \alpha \text{sat}\left(\frac{|x_{1,k}|}{\gamma h^2}\right)^{\frac{1}{2}} [x_{1,k}]^{\frac{1}{2}} \\ x_{2,k+1} &= x_{2,k} - h \beta \text{sat}\left(\frac{|x_{1,k}|}{\gamma h^2}\right) [x_{1,k}]^0, \end{aligned} \quad (16)$$

with $x_{1,k} = z_{0,k} - f_{0,k}$ and $x_{2,k} = z_{1,k} - f_{1,k}$.

Therefore, by setting $u_k = -\alpha \text{sat}\left(\frac{|x_{1,k}|}{\gamma h^2}\right)^{\frac{1}{2}} [x_{1,k}]^{\frac{1}{2}} + h \beta \text{sat}\left(\frac{|x_{1,k}|}{\gamma h^2}\right) + v_{k+1}$, $v_{k+1} = v_k - h \beta \text{sat}\left(\frac{|x_{1,k}|}{\gamma h^2}\right)$, the closed-loop dynamics of system (10) will follow the dynamics (16), which yields the controller functions in (8). This controller has a third tuning parameter γ . System (16) is linear in the band of the saturation around the origin. So, a natural choice of γ is such that the eigenvalues of this linear system are in the unit disk. This can be achieved by e.g. selecting $\gamma = G \begin{cases} \beta^2/\alpha^2 & \text{if } \alpha < 2\sqrt{\beta} \\ \alpha^2/4 & \text{else,} \end{cases}$ with $G > 1$ which is used in

Sections II and IV with $G = 1.5^2/1.1^2 \approx 1.8595$. This value was chosen, as for the relation $\alpha = 1.5\sqrt{\Lambda}$, $\beta = 1.1\Lambda$ this yields $\gamma = L$, respective $k_L = 1$, which is the recommended parameter value in [12].

APPENDIX B

PROOF OF THEOREM 2

If $x_k \in \mathcal{M}$ for some k , then Proposition 1 applies, and x_k remains in \mathcal{M} . Otherwise it is proven that x_k converges to \mathcal{M} in finite time. In the following, it is assumed that $x_k \notin \mathcal{M}$. Inspired by the stability analysis in [11, Theorem IV.1] define the Lyapunov candidate $V_k = 2\beta|x_{1,k} - h x_{2,k}| + x_{2,k}^2$. In general, using (4) the next step of the Lyapunov candidate computes to $V_{k+1} = 2\beta|x_{1,k} - h \alpha \Psi_1(x_{1,k})| + (x_{2,k} - h \beta \Psi_2(x_{1,k}) + h \Delta_k)^2$. For the proposed controller, this yields

$$\begin{aligned} V_{k+1} &= 2\beta \left| x_{1,k} - h^2 \beta \text{sat}\left(\frac{x_{1,k}}{h^2 \beta}\right) - h \alpha \text{sign}(x_{1,k}) \right| \\ &\quad \cdot \left(-\frac{h \alpha}{2} + \sqrt{\frac{h^2 \alpha^2}{4} + \max(0, |x_{1,k}| - h^2 \beta)} \right) + \\ &\quad + \left(x_{2,k} - h \beta \text{sat}\left(\frac{x_{1,k}}{h^2 \beta}\right) + h \Delta_k \right)^2. \end{aligned}$$

Case 1: $|x_{1,k}| \leq h^2 \beta$ gives

$$\begin{aligned} V_{k+1} &= 2\beta \left| x_{1,k} - x_{1,k} - h \alpha \text{sign}(x_{1,k}) \left(-\frac{h \alpha}{2} + \sqrt{\frac{h^2 \alpha^2}{4}} \right) \right| \\ &\quad + \left(x_{2,k} - \frac{1}{h} x_{1,k} + h \Delta_k \right)^2 = \left(x_{2,k} - \frac{1}{h} x_{1,k} + h \Delta_k \right)^2. \end{aligned}$$

The difference $\Delta V_k = V_{k+1} - V_k$ then computes to

$$\begin{aligned}\Delta V_k &= -2\beta|x_{1,k} - hx_{2,k}| + \left(x_{2,k} - \frac{1}{h}x_{1,k} + h\Delta_k\right)^2 - x_{2,k}^2 = \\ &= -2\beta|x_{1,k} - hx_{2,k}| + \frac{x_{1,k}^2}{h^2}(x_{1,k} - hx_{2,k}) - \frac{x_{1,k}x_{2,k}}{h} + \\ &\quad + h^2\Delta_k^2 - 2\Delta_k(x_{1,k} - hx_{2,k}) \\ &\leq (-\beta + 2L)|x_{1,k} - hx_{2,k}| - \frac{x_{1,k}x_{2,k}}{h} + h^2L^2,\end{aligned}$$

with the limit established with $|x_{1,k}| \leq h^2\beta$ and $|\Delta_k| \leq L$. From $x_k \notin \mathcal{M}$ and $|x_{1,k}| \leq h^2\beta$ follows $|x_{1,k+1}| = |x_{1,k} - hx_{2,k}| > h^2\beta$ and $|x_{2,k}| > 0$. Two cases are distinguished.

Case 1.a: $\text{sign}(x_{1,k}) = \text{sign}(x_{2,k})$ or $x_{1,k} = 0$ yields

$$\begin{aligned}\Delta V_k &\leq (-\beta + 2L)\underbrace{|x_{1,k} - hx_{2,k}|}_{>h^2\beta} - \frac{|x_{1,k}x_{2,k}|}{h} + h^2L^2 \leq \\ &\leq (-\beta + 2L)h^2\beta + h^2L^2 = h^2(L^2 - \beta^2 + 2L\beta) < 0,\end{aligned}$$

where the last inequality is fulfilled due to $\beta > 4L$.

Case 1.b: $\text{sign}(x_{1,k}) = -\text{sign}(x_{2,k})$ and $x_{1,k} \neq 0$

This case gives $|x_{1,k} - hx_{2,k}| > |hx_{2,k}|$. Assume $L = 0$. Then, with $|x_{1,k}| \leq h^2\beta$

$$\Delta V_k < -h\beta|x_{2,k}| + \frac{|x_{1,k}x_{2,k}|}{h} \leq -h\beta|x_{2,k}| + h\beta|x_{2,k}| = 0.$$

Now, assume $L > 0$, which gives with $H := -\frac{h^2\alpha^2}{2} + \sqrt{\frac{h^4\alpha^4}{4} + h^2\alpha^2(|x_{1,k+1}| - h^2\beta)} > 0$

$$\begin{aligned}V_{k+2} &= 2\beta\left|x_{1,k+1} - h^2\beta - H\right| + (x_{2,k+1} - \lfloor x_{1,k+1} \rfloor^0 h\beta)^2 + \\ &\quad + 2\Delta_{k+1}(hx_{2,k+1} - \lfloor x_{1,k+1} \rfloor^0 h^2\beta) + h^2\Delta_{k+1}^2.\end{aligned}$$

With $x_{1,k+1} = -x_{1,k} + hx_{2,k}$ and $x_{2,k+1} = -\frac{x_{1,k}}{h} + x_{2,k} + h\Delta_k$ from (14) and $\lfloor x_{1,k+1} \rfloor^0 = -\lfloor x_{1,k} \rfloor^0$ from $\text{sign}(x_{1,k}) = -\text{sign}(x_{2,k})$ this further computes to

$$\begin{aligned}V_{k+2} &= 2\beta\left|-x_{1,k} - h|x_{2,k}| + h^2\beta + H\right| + \\ &\quad + \left(-\frac{x_{1,k}}{h} + x_{2,k} + \lfloor x_{1,k} \rfloor^0 h\beta + h\Delta_k\right)^2 + \\ &\quad + 2\Delta_{k+1}(-x_{1,k} + hx_{2,k} + \lfloor x_{1,k} \rfloor^0 h^2\beta + h^2\Delta_k) + h^2\Delta_{k+1}^2\end{aligned}$$

Without loss of generality assume $x_{1,k} > 0$, i.e. $x_{2,k} < 0$, in the remaining part of this case. Thus, with $|\Delta_k| \leq L$, $|\Delta_{k+1}| \leq L$ and $-x_{1,k} + hx_{2,k} + h^2\beta < 0$ the upper limit

$$\begin{aligned}V_{k+2} &\leq 2\beta\left|hx_{2,k} - x_{1,k} + h^2\beta + H\right| + \left(x_{2,k} - \frac{x_{1,k}}{h} + h\beta - hL\right)^2 - \\ &\quad - 2L(hx_{2,k} - x_{1,k} + h^2\beta - h^2L) + h^2L^2\end{aligned}$$

is established. It can easily be shown that $-x_{1,k} + hx_{2,k} + h^2\beta + H < 0$. With some rearranging steps this gives

$$\begin{aligned}V_{k+2} - V_k &\leq -2\beta(h^2\beta + H) + \frac{x_{1,k}^2}{h^2} + 2\frac{|x_{1,k}x_{2,k}|}{h} + \\ &\quad + (\beta - L)\left(-2x_{1,k} + 2hx_{2,k} + h^2\beta - h^2L\right) + \\ &\quad + L2x_{1,k} - L2hx_{2,k} - L2h^2\beta + L3h^2L.\end{aligned}$$

With $|x_{1,k}| \leq h^2\beta$ and using the last expression the difference is further limited by

$$\begin{aligned}V_{k+2} - V_k &\leq -2\beta(h^2\beta + H) + \beta x_{1,k} - 2h\beta x_{2,k} + \\ &\quad + 2(\beta - 2L)(hx_{2,k} - x_{1,k}) + h^2\beta(\beta - 3L) - h^2L(\beta - 4L).\end{aligned}$$

Using $2(\beta - 2L) = (\beta - 3L) + \beta - L$ the last expression can be rewritten as

$$\begin{aligned}V_{k+2} - V_k &\leq -2\beta(h^2\beta + H) + Lx_{1,k} - h(\beta + L)x_{2,k} + \\ &\quad + (\beta - 3L)(-x_{1,k} + hx_{2,k} + h^2\beta) - h^2L(\beta - 4L).\end{aligned}$$

Due to $\beta > 4L$ the term $h^2L(\beta - 4L) < 0$, and due to $x_k \notin \mathcal{M}$ the term $(\beta - 3L)(-x_{1,k} + hx_{2,k} + h^2\beta) < 0$. It must be shown that the sum of the remaining terms is negative, i.e. $2\beta H \geq -2h^2\beta^2 + Lx_{1,k} - h(L + \beta)x_{2,k}$. This is trivial if the right-hand side is negative or zero, i.e. $|x_{2,k}| \leq \frac{h\beta(2\beta-L)}{\beta+L}$. It holds that $|x_{2,k}| \leq \sqrt{V_k} \leq \sqrt{V_0} \leq \sqrt{V}$. With $\beta > 4L$ and $\beta > \frac{5}{7}\frac{\sqrt{V}}{h}$ we have $|x_{2,k}| \leq \sqrt{V} < \frac{7}{5}h\beta \leq \frac{h\beta(2\beta-L)}{\beta+L}$ which was to be shown. Therefore $V_{k+2} < V_k$.

Case 2: $|x_{1,k}| > h^2\beta$ yields

$$\begin{aligned}V_{k+1} &= 2\beta\left|x_{1,k} - \text{sign}(x_{1,k})\left(h^2\beta + h\alpha\left(-\frac{h\alpha}{2} + \sqrt{\frac{h^2\alpha^2}{4} + |x_{1,k}| - h^2\beta}\right)\right)\right| + \\ &\quad + (x_{2,k} - \text{sign}(x_{1,k})h\beta)^2 - \\ &\quad - 2\Delta_k(x_{2,k} - \text{sign}(x_{1,k})h\beta) + h^2\Delta_k^2.\end{aligned}$$

Let us introduce $z_{1,k} := x_{1,k} - \text{sign}(x_{1,k})h^2\beta$, $z_{2,k} := x_{2,k} - \text{sign}(x_{1,k})h\beta$, with $z_{1,k} \in \mathbb{R} \setminus \{0\}$ and $z_{2,k} \in \mathbb{R}$. Note that $\text{sign}(x_{1,k}) = \text{sign}(z_{1,k})$. This gives

$$\begin{aligned}V_k &= 2\beta|z_{1,k} - hz_{2,k}| + z_{2,k}^2 + \text{sign}(z_{1,k})2h\beta z_{2,k} + h^2\beta^2, \\ V_{k+1} &= 2\beta\left|z_{1,k} - h\alpha\text{sign}(z_{1,k})\left(-\frac{h\alpha}{2} + \sqrt{\frac{h^2\alpha^2}{4} + |z_{1,k}|}\right)\right| + \\ &\quad + z_{2,k}^2 - 2\Delta_k z_{2,k} + h^2\Delta_k^2,\end{aligned}$$

and further with $A := h\alpha\left(-\frac{h\alpha}{2} + \sqrt{\frac{h^2\alpha^2}{4} + |z_{1,k}|}\right) > 0$

$$\begin{aligned}\Delta V_k &= 2\beta(|z_{1,k} - \text{sign}(z_{1,k})A| - |z_{1,k} - hz_{2,k}|) \\ &\quad - 2h\beta\text{sign}(z_{1,k})z_{2,k} - h^2\beta^2 + h^2\Delta_k^2 - 2\Delta_k z_{2,k} \\ &\leq 2\beta(|z_{1,k} - \text{sign}(z_{1,k})A| - |z_{1,k} - hz_{2,k}|) \\ &\quad + 2L|z_{2,k}| - 2h\beta\text{sign}(z_{1,k})z_{2,k} - h^2\beta^2 + h^2L^2\end{aligned}$$

Note that this upper limit of ΔV_k is an even function. Therefore, it is sufficient to only consider the case $z_{1,k} > 0$. The following shows that $z_{1,k} - A \geq 0$ always holds, as

$$\left(z_{1,k} + \frac{h^2\alpha^2}{2}\right)^2 \geq \left(\frac{h^4\alpha^4}{4} + h^2\alpha^2 z_{1,k}\right) \Leftrightarrow z_{1,k}^2 \geq 0,$$

which holds $\forall z_{1,k}$. Together this yields

$$\begin{aligned}\Delta V_k &\leq 2\beta((z_{1,k} - A) - |z_{1,k} - hz_{2,k}|) - 2h\beta z_{2,k} \\ &\quad + 2L|z_{2,k}| - h^2\beta^2 + h^2L^2,\end{aligned}$$

and is assumed in the remaining part of the proof. Two cases are distinguishing in the following.

Case 2.a: $z_{1,k} - hz_{2,k} \geq 0$ leads to

$$\begin{aligned} \Delta V_k &\leq 2\beta(hz_{2,k} - A - hz_{2,k}) + 2L|z_{2,k}| - h^2(\beta^2 - L^2) \\ &= -2\beta A + 2L|z_{2,k}| - h^2(\beta^2 - L^2) \leq 2L|z_{2,k}| - h^2(\beta^2 - L^2), \end{aligned} \quad [14]$$

which must be negative. For $L = 0$ this is fulfilled. For $L > 0$ and with $|z_{2,k}| \leq \sqrt{V_k} < \sqrt{V}$ it is sufficient that $2L\sqrt{V} < h^2(\beta^2 - L^2)$, which is fulfilled due to $\beta^2 > L^2 + \frac{2L\sqrt{V}}{h^2}$ and thus $\Delta V_k < 0$.

Case 2.b: $z_{1,k} - hz_{2,k} < 0$ gives $z_{2,k} > 0$ and

$$\begin{aligned} \Delta V_k &\leq 2\beta(2z_{1,k} - A - hz_{2,k}) + 2(L - h\beta)z_{2,k} - h^2\beta^2 + h^2L^2 \\ &= 4\beta(z_{1,k} - hz_{2,k}) - 2\beta A + 2Lz_{2,k} - h^2(\beta^2 - L^2) \\ &\leq 2Lz_{2,k} - h^2(\beta^2 - L^2), \end{aligned}$$

which was already shown in Case 2.a to be negative.

In the cases above all possible combinations of states $(x_{1,k}, x_{2,k})$ were considered. In all cases but Case 1.b $(x_{1,k}, x_{2,k}) \notin \mathcal{M}$, $\Delta V_k(x_{1,k}, x_{2,k}) < 0$ was proven. In Case 1.b $V_{k+2} - V_k < 0$ was proven. Therefore, $\Delta V_{2,k} := V_{k+2} - V_k = \Delta V_{k+1} + \Delta V_k < 0$. V_k is continuous in $(x_{1,k}, x_{2,k})$ and as ΔV_k is continuous, also $\Delta V_{2,k}$ is continuous. Due to the continuity the maximum of $\Delta V_{2,k}$ exists. Further $V_k > 0 \forall x_k \neq 0$ and $V_k = 0$ for $x_k = 0$. So, $\exists V_M > 0$ such that $x_k \notin \mathcal{M} \Rightarrow V_k > V_M$. Thus, $\exists \delta := \max_{x_k \notin \mathcal{M}, V_k \leq V} (\Delta V_{2,k}) < 0$ and so the maximum number of steps until \mathcal{M} is reached, $(V_0 - V_M)/|\delta| < \infty$, is finite. Therefore, x_k converges to \mathcal{M} in a finite number of steps, i.e. in finite time.

REFERENCES

- [1] Y. Shtessel, C. Edwards, L. Fridman, and A. Levant, *Sliding Mode Control and Observation*. Birkhauser, 2013, p. 356.
- [2] V. Acary, B. Brogliato, and Y. V. Orlov, "Chattering-free digital sliding-mode control with state observer and disturbance rejection," *IEEE Transactions on Automatic Control*, vol. 57, no. 5, pp. 1087–1101, 2012.
- [3] A. Levant, "Discretization issues of high-order sliding modes," *IFAC Proceedings Volumes*, vol. 44, no. 1, pp. 1904–1909, 2011.
- [4] V. Acary and B. Brogliato, "Implicit Euler numerical scheme and chattering-free implementation of sliding mode systems," *Systems & Control Letters*, vol. 59, no. 5, pp. 284–293, 2010.
- [5] A. Levant, "Sliding order and sliding accuracy in sliding mode control," *International Journal of Control*, vol. 58, no. 6, pp. 1247–1263, 1993.
- [6] J. A. Moreno and M. Osorio, "Strict Lyapunov Functions for the Super-Twisting Algorithm," *IEEE Transactions on Automatic Control*, vol. 57, no. 4, pp. 1035–1040, 2012.
- [7] Y. Chen, H. Dong, J. Lu, X. Sun, and L. Guo, "A Super-Twisting-Like Algorithm and Its Application to Train Operation Control With Optimal Utilization of Adhesion Force," *IEEE Transactions on Intelligent Transportation Systems*, vol. 17, no. 11, pp. 3035–3044, 2016.
- [8] A. D. Pizzo, L. P. D. Noia, and S. Meo, "Super twisting sliding mode control of smart-inverters grid-connected for PV applications," in *IEEE International Conference on Renewable Energy Research and Applications*, 2017, pp. 793–796.
- [9] B. Brogliato, A. Polyakov, and D. Efimov, "The implicit discretization of the super-twisting sliding-mode control algorithm," in *IEEE International Workshop on Variable Structure Systems*, 2018, pp. 349–353.
- [10] X. Xiong, G. Chen, Y. Lou, R. Huang, and S. Kamal, "Discrete-Time Implementation of Super-Twisting Control With Semi-Implicit Euler Method," *IEEE Transactions on Circuits and Systems II: Express Briefs*, vol. 69, no. 1, pp. 99–103, 2022.
- [11] S. Koch, M. Reichhartinger, and M. Horn, "On the Discretization of the Super-Twisting Algorithm," in *IEEE Conference on Decision and Control*, 2019, pp. 5989–5994.
- [12] A. Hanan, A. Levant, and A. Jbara, "Low-Chattering Discretization of Homogeneous Differentiators," *IEEE Transactions on Automatic Control*, vol. 67, no. 6, pp. 2946–2956, 2022.
- [13] V. Utkin, "On convergence time and disturbance rejection of super-twisting control," *IEEE Transactions on Automatic Control*, vol. 58, no. 8, pp. 2013–2017, 2013.
- [14] M. Livne and A. Levant, "Proper discretization of homogeneous differentiators," *Automatica*, vol. 50, no. 8, pp. 2007–2014, 2014.
- [15] L. Fridman, J. Moreno, and R. Iriarte, Eds., *Sliding Modes after the First Decade of the 21st Century*. Springer Berlin Heidelberg, 2012.
- [16] B. Brogliato, A. Polyakov, and D. Efimov, "The Implicit Discretization of the Supertwisting Sliding-Mode Control Algorithm," *IEEE Transactions on Automatic Control*, vol. 65, no. 8, pp. 3707–3713, 2020.
- [17] S. Koch and M. Reichhartinger, "Discrete-time equivalents of the super-twisting algorithm," *Automatica*, vol. 107, pp. 190–199, 2019.
- [18] A. Emami-Naeini and G. Franklin, "Deadbeat control and tracking of discrete-time systems," *IEEE Transactions on Automatic Control*, vol. 27, no. 1, pp. 176–181, 1982.